

# Fast radio bursts: search sensitivities and completeness

E. F. Keane<sup>1,2★</sup> and E. Petroff<sup>1,2,3</sup>

<sup>1</sup>Centre for Astrophysics and Supercomputing, Swinburne University of Technology, Mail H29, PO Box 218, VIC 3122, Australia

<sup>2</sup>ARC Centre of Excellence for All-sky Astrophysics (CAASTRO)

<sup>3</sup>CSIRO Astronomy & Space Science, Australia Telescope National Facility, PO Box 76, Epping, NSW 1710, Australia

Accepted 2014 December 12. Received 2014 November 27; in original form 2014 September 22

## ABSTRACT

In this paper we identify some sub-optimal performance in algorithms that search for fast radio bursts (FRBs), which can reduce the cosmological volume probed by over 20 per cent, and result in missed discoveries and incorrect flux density and sky rate determinations. Re-calculating parameters for all of the FRBs discovered with the Parkes telescope (i.e. all of the reported FRBs bar one), we find some inconsistencies with previously determined values, e.g. FRB 010125 was approximately twice as bright as previously reported. We describe some incompleteness factors not previously considered which are important in determining accurate population statistics, e.g. accounting for fluence incompleteness the Thornton et al. all-sky rate can be re-phrased as  $\sim 2500$  FRBs per sky per day above a 1.4-GHz fluence of  $\sim 2$  Jy ms. Finally we make data for the FRBs easily available, along with software to analyse these.

**Key words:** methods: data analysis – surveys – intergalactic medium.

## 1 INTRODUCTION

Fast radio bursts (FRBs) are millisecond-duration jansky-flux density signals which have been discovered by single dish radio telescopes operating at frequencies of  $\sim 1.4$  GHz (Lorimer et al. 2007; Keane et al. 2011; Thornton et al. 2013; Burke-Spolaor & Bannister 2014; Petroff et al. 2014b; Spitler et al. 2014). All but one of the nine reported events have been detected with the 64-m Parkes Telescope; the other with the 300-m dish at Arecibo. The bursts exhibit a frequency-dependent time delay which obeys a quadratic form so strictly that the signals could only have traversed low-density regions, such as the interstellar and intergalactic media, en route to Earth (Dennison 2014). The magnitude of this delay – parametrized by the dispersion measure (DM), which is the integrated electron density along the line of sight – is so large that cosmological distances are inferred for the sources of the FRBs (Ioka 2003; Inoue 2004). Because of this the potential astrophysical/cosmological uses of FRBs are numerous, and include weighing the ‘missing baryons’ (McQuinn 2014), measuring the intergalactic magnetic field and determining the dark energy equation of state (Gao, Li & Zhang 2014; Zhou et al. 2014).

In this paper we present, in Section 2, an assessment of the search algorithms used to discover FRBs, highlighting some key concerns where sensitivity to FRBs is often unnecessarily reduced, and how this can be avoided. In Section 3, we re-calculate some basic parameters for all of the Parkes FRBs in a self-consistent manner. These serve as input to Section 4, where we describe some

incompleteness issues in our sampling of the FRB population. In Section 5, we then make our conclusions.

## 2 SINGLE PULSE SEARCHES

Thus far, FRBs have been detected in beam-formed radio observations as follows. (i) *Acquisition*: radio telescopes record incoherent filterbank data; these are time-frequency-flux density data cubes. Thus far, the data wherein FRBs have been discovered have been centred at  $\sim 1.4$  GHz with bandwidths ranging from 288 to 400 MHz, frequency resolutions ranging from 0.336 to 3 MHz and time resolutions ranging from 0.064 to 1 ms. (ii) *Cleaning*: the data are cleaned of radio frequency interference signals in various ways. (iii) *Dedispersion*: the data are dedispersed at a number of trial DM values to remove frequency-dependent delays imparted by the interstellar and intergalactic media. (iv) *Search*: each dedispersed time series is subjected to a single pulse (SP) search, which is a matched filter search to a number of trial boxcar widths. Usually events down to a level which is well within the noise floor are recorded. (v) *Refinement*: upon detection optimised DM and width values of the pulse are derived.

In steps (ii)–(iv) there is the potential for a loss in sensitivity. All of these are avoidable, but accuracy is sometimes sacrificed for processing speed. The DM parameter is always covered in a ‘scaloped’ fashion, where the next DM trial is chosen so as to limit the sensitivity loss of a narrow pulse falling between DM trials. Typically the choice is to lose no more than  $\sim 10$  per cent of the sensitivity for bursts narrower than the sampling time. However, FRBs are typically much wider than the sampling time, and the observed width is dominated by dispersion smearing so that the

\* E-mail: [Evan.Keane@gmail.com](mailto:Evan.Keane@gmail.com)

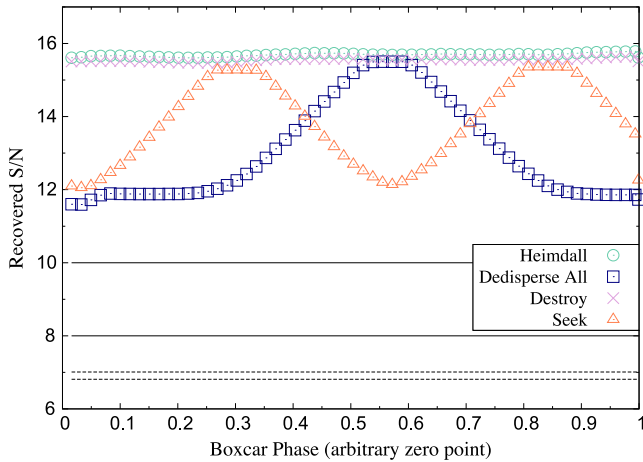


**Figure 1.** Here we show the detected S/N of a simulated FRB (intrinsic pulse width 2 ms, DM of  $1000 \text{ cm}^{-3} \text{ pc}$  observed at  $\sim 1.4 \text{ GHz}$ ) for four commonly used SP search codes, as a function of ‘boxcar phase’. The injected S/N in this case is 16. Due to dispersion smearing, and searching for power-of-2 boxcars the maximum theoretical detection S/N is 15.4. Here we plot the mean recovered S/N values for 100 random realizations. We can see that HEIMDALL (circles) and DESTROY (crosses) recover the correct S/N regardless of the position of the phase. DEDISPERSER\_ALL (squares) and SEEK (triangles) give S/N values which are strongly dependent on phase, with a maximum loss factor of  $\sim \sqrt{2}$ . The rms deviation of the recovered S/N values (not shown) are in all cases  $\sim 1$ , as expected. Also shown are various thresholds: a  $10\sigma$  threshold which is often used for real time FRB searches (Petroff et al. 2014b), an  $8\sigma$  threshold more commonly used for offline processing, two ‘false-alarm’ thresholds for typical pulsar search parameters: the lower (higher) dashed line for observations with  $2^{21}$  ( $2^{23}$ ) samples, 1000 DM trials and 10 width trials.

loss in sensitivity to FRBs is typically much less than this. As DM corresponds to the volume probed in a line-of-sight-dependent way, the actual volume probed can be quite uncertain, especially for lines-of-sight closer to the Galactic plane.

The searching step can be subject to the ‘root 2 problem’, which manifests itself when performing a ‘decimation search’. This is a procedure in which a time series is searched for events of 1 sample in width. It is then down-sampled by a factor of 2, averaging adjacent samples. This process is repeated a number of times in order to search for a range of pulse widths (Cordes & McLaughlin 2003). However, this search method is not optimal. For example, let us consider a time series with samples  $i$ ,  $i = 1, 2, 3, 4, \dots$ , and a top-hat pulse which is four bins wide, occupying bins 3, 4, 5 and 6. This pulse is ‘out of phase’ with respect to the down-sampling procedure and it is clear that the derived S/N will be too low by a factor of  $\sqrt{2}$ . The optimal way to search a time series is to run a sliding boxcar along the time series.

Fig. 1 illustrates this problem by showing the results of searching for a synthesized FRB as it is moved along a time series in single time sample steps up to one pulse width in total. The results of several commonly used SP search codes are shown. In particular these are HEIMDALL,<sup>1</sup> DEDISPERSER\_ALL,<sup>2</sup> SEEK<sup>2</sup> and DESTROY.<sup>3</sup> Here a ‘typical’ FRB with an intrinsic pulse width of 2 ms (16 bins for the simulated time sampling value of 125  $\mu\text{s}$ ), a DM of  $1000 \text{ cm}^{-3} \text{ pc}$ , and an injected S/N of 16, is used. The data are centred at a

frequency of 1374 MHz with spectral resolution of 3 MHz meaning the dispersion smearing will make the observed pulse width 7.4 ms (59 bins). Thus, for a power-of-2 boxcar search the optimal S/N we expect to find is  $16 \max(\sqrt{32/59}, \sqrt{59/64}) = 16\sqrt{59/64} = 15.4$ .

We can see that DEDISPERSER\_ALL reaches the maximum theoretical S/N when the pulse is ‘in phase’ and reaches a minimum S/N when the pulse is ‘out of phase’. SEEK has the same problem, although to a lesser extent, and is relatively rotated in phase and with a response curve which repeats at twice the frequency. These differences are because SEEK performs an extra 2-bin smoothing step to the data prior to each down-sampling step. HEIMDALL and DESTROY give the correct result for all ‘phases’. We have verified that the curves in Fig. 1 scale directly with the injected S/N. One can quickly make a very simplified estimate of the effects of these results on a survey, e.g. for an  $N \propto S_{\text{min}}^{-3/2}$  law SEEK probes 86 per cent and DEDISPERSER\_ALL only 78 per cent of the volume probed by HEIMDALL and DESTROY. The true volume probed will be slightly lower than this however as here the exact DM of the pulse has been used, so that the ‘scallop’ loss factor (which would affect all four codes equally) has been removed. Crucially this can mean that FRBs detectable in our data are never detected. Some of these errors can also result in incorrect flux density and volumetric rate estimates for those FRBs which are detected.

### 3 THE PARKES FRBS

The eight Parkes FRBs were discovered using different search software packages – Lorimer et al. (2007) used SEEK, Keane et al. (2011) used DESTROY, both Thornton et al. (2013) and Burke-Spolaor & Bannister (2014) used DEDISPERSER\_ALL, and Petroff et al. (2014b) used HEIMDALL. Because of this, and the issues highlighted in Section 2, previously reported parameters like the observed flux densities, widths and fluence (and hence derived parameters like the energy released in the FRB event) may be incorrect. We have therefore re-determined the signal-to-noise ratios (S/N) and observed widths of all of the Parkes FRBs in a self-consistent way, and hence determined the observed flux densities and fluences. The results of these calculations are tabulated in Table 1.

We report higher values of S/N and width for FRB 010724 and the four Thornton bursts. For the latter the average reduction in S/N is consistent with the average of the DEDISPERSER\_ALL response curve in Fig. 1. It is certainly conceivable that other FRBs, especially weaker events, were missed in the Thornton et al. (2013) search, which motivates a complete re-processing of the high Galactic latitude component of the High Time Resolution Universe survey, as recently done for the intermediate latitude component (Petroff et al. 2014a). Such a search is in fact currently underway (Champion et al. in preparation). We also estimate that FRB 010125 was twice as bright as initially reported. Some of this difference is attributable to the use of the full width at half-maximum by Burke-Spolaor & Bannister (2014), with a factor of  $\sqrt{2}$  discrepancy in the S/N which we postulate to be due to the root 2 problem.

In addition to the measured parameters we can determine a number of model-dependent quantities, and several of these are listed in Table 2. Throughout we include FRB 010621 in our analyses but note that this event has a very high probability of being Galactic in origin (Keane et al. 2012; Bannister & Madsen 2014): we use this to gauge a reasonable uncertainty in the maximum Milky Way contribution to each event’s DM. Subtracting this contribution one can invoke a model relating DM and redshift (Ioka 2003; Inoue 2004) to derive an upper limit redshift estimate for each event. Unlike Thornton et al. (2013) we do not subtract a putative host

<sup>1</sup> <http://sourceforge.net/projects/heimdall-astro/>

<sup>2</sup> see e.g. <https://github.com/SixByNine/prsoft>.

<sup>3</sup> [https://github.com/evanocathain/destroy\\_gutted](https://github.com/evanocathain/destroy_gutted)

**Table 1.** This table summarizes some of the measured parameters for the Parkes FRBs (where the date IDs have been corrected where appropriate), with the reported values for the Arecibo FRB also listed for reference. Those FRBs discovered using the analogue filterbanks (AFBs,  $96 \times 3$  MHz bandwidth) at Parkes are marked with a † and those discovered with the Berkeley-Parkes-Swinburne Recorder (BPSR,  $1024 \times 0.390\,625$  MHz bandwidth) are marked with a ♣. All Parkes events were discovered using the 13-beam receiver, where the central and most sensitive beam is surrounded by two ever less sensitive hexagonal rings of six beams (Staveley-Smith et al. 1996). The beam number wherein each burst was detected is given. The published DM values are followed by the S/N as calculated by DESTROY. The observed width is that which gives the maximum S/N value. In the case of the beam 6 detection of FRB 010724 the 1-bit digitizers saturated so that the S/N listed is a lower limit. The observed peak flux density is calculated using the listed S/N and width values, a system temperature of 28 K (Parkes Observing Guide, 2014 Sep Edition), the usable bandwidth after RFI-affected channels are removed (conservatively this is 261 MHz for the AFBs and 338.281 25 MHz for BPSR), the relevant digitization loss factor (AFB: 0.798, BPSR: 0.936), and the relevant beam-dependent gain factor (Manchester et al. 2001). The observed fluence is simply the product of the width and the peak flux density values. The true peak flux density and fluence values are higher than the observed values by  $1/G(\theta)$ , the inverse of the angular response of the beam: the mean of this boost factor is  $\sim 2$  (Macquart, private communication). Note that the time sampling used varied: FRB 010125, FRB 010621, and FRB 010724 were observed with time resolutions of 0.125, 0.250, and 1.000 ms, respectively, whereas all of the BPSR detections had time resolution of 0.064 ms. References correspond to [1] Burke-Spolaor & Bannister (2014) [2] Keane et al. (2012) [3] Lorimer et al. (2007) [4] Thornton et al. (2013) [5] Petroff et al. (2014b) [6] Spitler et al. (2014).

Event	Parkes beam ID	DM ( $\text{cm}^{-3}$ pc)	S/N	$W_{\text{obs}}$ (ms)	$S_{\text{peak,obs}}$ (Jy)	$F_{\text{obs}}$ (Jy ms)	Ref.
Parkes FRBs							
FRB 010125†	5	790(3)	25(1)	$10.3^{+2.9}_{-2.5}$	$0.55^{+0.11}_{-0.08}$	$5.6^{+3.0}_{-2.0}$	[1]
FRB 010621†	10	746(1)	18(1)	$8.3^{+4.0}_{-2.3}$	$0.52^{+0.13}_{-0.11}$	$4.3^{+3.6}_{-1.9}$	[2]
FRB 010724†	6	375(1)	>100	$\sim 20$	>1.58	>31.5	[3]
	7	375(1)	16(1)	$9^{+12}_{-2}$	$0.38^{+0.07}_{-0.15}$	$3.4^{+6.1}_{-1.8}$	
	12	375(1)	6(1)	$33^{+12}_{-28}$	$0.09^{+0.17}_{-0.03}$	$2.9^{+8.9}_{-2.6}$	
	13	375(1)	27(1)	$15^{+4}_{-3}$	$0.58^{+0.10}_{-0.08}$	$8.7^{+4.1}_{-2.7}$	
FRB 110220♣	3	944.38(5)	54(1)	$6.6^{+1.3}_{-1.0}$	$1.11^{+1.12}_{-0.10}$	$7.3^{+2.4}_{-1.7}$	[4]
FRB 110626♣	12	723.0(3)	12(1)	$1.4^{+1.2}_{-0.4}$	$0.63^{+0.20}_{-0.13}$	$0.9^{+1.3}_{-0.4}$	[4]
FRB 110703♣	5	1103.6(7)	17(1)	$3.9^{+2.2}_{-1.9}$	$0.45^{+0.21}_{-0.10}$	$1.8^{+2.3}_{-1.1}$	[4]
FRB 120127♣	4	553.3(3)	13(1)	$1.2^{+0.6}_{-0.3}$	$0.62^{+0.13}_{-0.10}$	$0.8^{+0.6}_{-0.3}$	[4]
FRB 140514♣	1	562.7(6)	16(1)	$2.8^{+3.5}_{-0.7}$	$0.47^{+0.11}_{-0.08}$	$1.3^{+2.3}_{-0.5}$	[5]
Arecibo FRB							
FRB 121102	n/a	557(2)	14(1)	3.0(5)	$0.4^{+0.4}_{-0.1}$	$1.2^{+4.0}_{-1.0}$	[6]

contribution as it adds to the number of assumptions needed (i.e. that there is a galactic host and that we must assume a knowledge of its composition). We also ignore the variance in the IGM-contributed DM (see McQuinn 2014), as, without independent redshift measurements, this has not yet been quantified. Based on the therefore rather crude redshift estimate we can derive comoving and luminosity distances in the standard cosmology (Wright 2006), and thence the energy released to produce the radio burst. The estimates for the energy cover a range of two orders of magnitude. Determining the rest-frame peak luminosity for both the upper limit on the intrinsic width (the observed width less the effects of dispersion smearing and, where observed, multipath scattering) and a rest-frame time-scale does not lessen this large range of values. The unknown angular offsets (which, if accounted for would boost the flux density and fluence), and the likely large variance from the average DM as a function of redshift, neither of which have we accounted for, will only increase the range. Thus we do not have enough precision in our measurements to determine if the FRBs are standard candles or not, even assuming the models we have applied here are accurate. As all values quoted in Table 2 are highly model-dependent and

subject to large uncertainties we suggest caution when using these values for population analyses.

#### 4 SELECTION EFFECTS IN FRB SEARCHES

The estimate for FRBs detectable by the current setup at Parkes is  $\sim 10^4$  FRBs per ( $4\pi$  sr) per day (Thornton et al. 2013). This number is simply the observed rate of four FRBs in 23 d, extrapolated, from the  $\sim 0.55$  deg<sup>2</sup> half-power field-of-view of the multibeam receiver at Parkes (Staveley-Smith et al. 1996), to the entire sky. In addition to the obvious caveats of such an extrapolation, the meaning of this rate must be interpreted carefully, for a number of reasons.

*Fluence & width incompleteness?* One might suggest that the all-sky rate is that above the flux-density threshold at the half-power beamwidth of Parkes. Even though the physically relevant parameter is the fluence, i.e. the area under the pulse curve in the dedispersed time series, our sensitivity depends also on the pulse width. Thus, pulses with the same fluence but different widths (due to traversing different paths in the IGM/ISM) are not equally detectable. Fig. 2 shows the sensitivity to bursts in the flux

**Table 2.** This table summarizes some of the model-dependent parameters derived from the measured values presented in Table 1.  $DM_{MW}$  is the maximum Milky Way contribution to the DM for the line of sight to the FRB according to the NE2001 model of the Galaxy’s free electron content (Cordes & Lazio 2002). The uncertainties on  $DM_{MW}$  are taken to be a factor of 2, enough to imply a Galactic origin for FRB 010621, as seems to be realistic (Keane et al. 2012; Bannister & Madsen 2014). This uncertainty propagates through to all the following derived parameters. The ratio of DM to  $DM_{MW}$  is also given, where a value greater than 1 nominally implies an extragalactic source. The redshift value is simply determined from  $z_{\text{model}} = (DM - DM_{MW})/1200$  (Ioka 2003; Inoue 2004). The comoving distance is determined using the calculator of Wright (2006). The luminosity distance is simply  $(1 + z)$  times the comoving distance. The energy is calculated as the product of the observed fluence, the blueshifted effective bandwidth of the observations, and the square of the luminosity distance. No assumption of isotropy is made, i.e. a beaming solid angle of 1 sr is used as per Thornton et al. (2013).

Event	$DM_{MW}$ ( $\text{cm}^{-3}$ pc)	$DM/DM_{MW}$	$z_{\text{model}}$	$D_{\text{comov}}$ (Gpc)	$D_L$ (Gpc)	Energy ( $10^{32}$ J)
Parkes FRBs						
FRB 010125 <sup>†</sup>	110	7.2	$< 0.57^{+0.04}_{-0.05}$	$< 2.1^{+0.12}_{-0.16}$	$< 3.4^{+0.3}_{-0.4}$	$< 2.5^{+2.1}_{-1.2}$
FRB 010621 <sup>†</sup>	523	1.4	$< 0.19^{+0.21}_{-0.19}$	$< 0.8(8)$	$< 0.9^{+1.3}_{-0.9}$	$< 0.1^{+1.3}_{-0.1}$
FRB 010724 <sup>†</sup>	45	8.4	$< 0.28^{+0.01}_{-0.02}$	$< 1.13^{+0.04}_{-0.08}$	$< 1.4(1)$	$< 2.1$
FRB 110220 <sup>♣</sup>	35	27.2	$< 0.76^{+0.01}_{-0.02}$	$< 2.71^{+0.03}_{-0.06}$	$< 4.8^{+0.1}_{-0.2}$	$< 9.4^{+0.6}_{-4.2}$
FRB 110626 <sup>♣</sup>	48	15.2	$< 0.56(2)$	$< 2.10^{+0.07}_{-0.06}$	$< 3.3^{+0.1}_{-0.2}$	$< 0.5^{+0.5}_{-0.3}$
FRB 110703 <sup>♣</sup>	32	34.1	$< 0.89^{+0.02}_{-0.01}$	$< 3.07^{+0.05}_{-0.03}$	$< 5.8(1)$	$< 3.6^{+3.2}_{-2.5}$
FRB 120127 <sup>♣</sup>	32	17.4	$< 0.43^{+0.02}_{-0.01}$	$< 1.67^{+0.07}_{-0.03}$	$< 2.4(1)$	$< 0.2(1)$
FRB 140514 <sup>♣</sup>	35	16.1	$< 0.44(1)$	$< 1.71^{+0.03}_{-0.03}$	$< 2.46^{+0.04}_{-0.06}$	$< 0.4^{+0.4}_{-0.2}$
Arecibo FRB						
FRB 121102	188	3.0	$< 0.31(8)$	$< 1.2(3)$	$< 1.6^{+0.5}_{-0.4}$	$< 0.133^{+0.674}_{-0.127}$

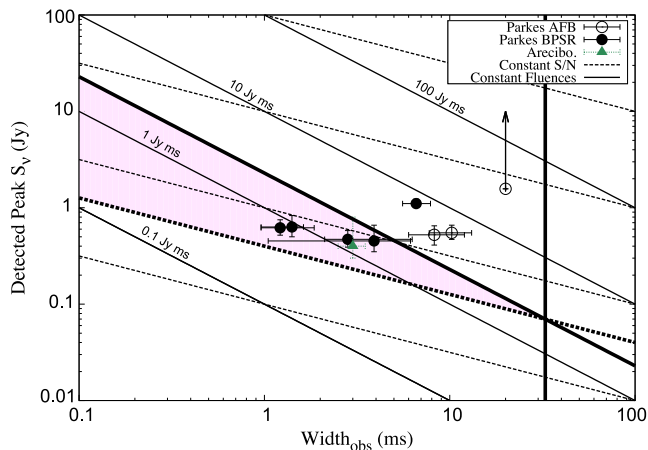


**Figure 2.** The detected flux density–observed width parameter space. Lines of constant S/N (dashed) and constant fluence (solid) are shown. Events above the thick dashed line are detectable at Parkes. In this case, and if all FRBs are less than some maximum putative width (here denoted by the thick vertical line), we only have fluence completeness above  $\sim 2$  Jy ms. In the shaded triangle we have fluence incompleteness. The Arecibo FRB (green triangle) is included for illustration only: different incompleteness regions apply to different observing configurations.

density–width plane. We are always incomplete to wide bursts. However, if FRBs do not exist above some maximum width,<sup>4</sup> we are still left with an incomplete sampling of fluence. This feeds into the often posed question of ‘what is the  $\log N$ – $\log S$  distribution?’. In this case, ‘ $S$ ’ ought to be fluence, and fluence completeness should

<sup>4</sup> The width of 32 ms used in Fig. 2 is the maximum to which FRB searches at Parkes are sensitive (Petroff et al. 2014a).

be accounted for. Considering Fig. 2, this would imply discarding half of the Parkes FRBs and then binning the remainder. With such a small number of detections this is not yet a meaningful exercise. Fluence completeness should be considered when determining population estimates.

*Latitude dependence?* Some additional selection effects have been identified empirically, e.g. FRBs seem to be much more difficult to detect at lower Galactic latitudes, despite intensive efforts (Burke-Spolaor & Bannister 2014; Petroff et al. 2014a). This points towards a Galactic obscuration effect but at present none of the known possibilities are sufficient to explain the paucity of low-latitude detections. The possibility remains that the rate (extrapolated from four events, see above) is in fact too high.

*What is an FRB?* There is also the question as to how to algorithmically define what an FRB is, in contrast to an ‘RRAT’: pulsars which show detectable SPs of radio emission only very occasionally (Keane & McLaughlin 2011). If we detect an SP from an RRAT how do we distinguish it from an FRB? An RRAT may eventually repeat but the main difference is that RRATs are Galactic whereas FRBs are believed to be extragalactic. We decide upon this based on the ratio of the DM of a detected event to the maximum Galactic DM contribution along the line of sight,  $DM_{MW}$ . If  $x = DM/DM_{MW} > 1$ , then the source is extragalactic, but the model we use to determine  $DM_{MW}$  is quite uncertain, especially at high Galactic latitudes (Cordes & Lazio 2002). This has resulted in ad hoc selection rules such as selecting events with  $x > 0.9$  (Petroff et al. 2014a), but, as noted in Spitler et al. (2014), there is a rather wide ‘grey area’ in this parameter space. As the uncertainty on  $x$  depends both on the DM and the line of sight in very systematic ways this is difficult to quantify and it is quite conceivable that many FRBs have already been detected and falsely labelled as RRATs, and the converse may already be the case for FRB 010621. In effect there is a low-redshift blindness to FRBs, analogous to the low-DM blindness in Galactic SP searches (Keane et al. 2010).

## 5 CONCLUSIONS

With so many selection effects evident, large uncertainties in flux density and fluence estimates (see Section 3), essentially no knowledge of FRB spectra, and when dealing with such small number statistics, serious population analyses are precluded. These obstacles will be overcome only when a much larger number of FRBs are discovered. For example, to remove the fluence incompleteness one could simply discard all FRBs below the incompleteness value. Considering the Thornton events, and under the assumption that no FRBs are broadened more than  $\approx 32$  ms, this means discarding three out of the four events and interpreting the Parkes FRB rate above a fluence of  $\sim 2$  Jy ms to be  $\sim 2500$  per sky per day. Clearly this estimate is hugely uncertain and such analyses will only become more practical (see Fig. 2) when a much larger sample is obtained and the population below the incompleteness boundary can be modelled. To remove the low-redshift blindness we might benefit from independent distance estimates. New means of estimating the distance, such as the method of Bannister & Madsen (2014), could shed some light on this if they are applied to a large sample of RRATs and FRBs. We encourage the community to search all ongoing and archival surveys for FRBs: given the issues raised in Section 2 we propose that this is best done using HEIMDALL, or one using the same search algorithm. Such searches could yield a few tens of new FRBs. Beyond that the only way to discover hundreds to thousands of FRBs is to use high-sensitivity wide field-of-view telescopes with a large amount of on-sky time, e.g. through ‘piggy-back’ transient observations with MeerKAT and SKA1-Mid (Fender 2015). This will be necessary to maximize the scientific return on yet-to-be detected FRBs (Petroff et al. 2014b).

## DATA AND SOFTWARE RELEASE

We have made the data easily available for the FRBs discussed in this paper. The data can be accessed via the Research Data Australia Portal.<sup>5</sup> Additionally analysis software is available and can be accessed via a GITHUB repository.<sup>6</sup> These have been used in the preparation of this paper. It is our hope that others can use these to directly access and analyse the raw data collected at the telescope.

<sup>5</sup> <http://researchdata.ands.org.au/fast-radio-bursts-parkes/>

<sup>6</sup> [https://github.com/evanocathain/Useful\\_FRB\\_stuff](https://github.com/evanocathain/Useful_FRB_stuff)

In this way uncertainties and misinterpretations can be minimized, and new predictions and analysis tools can be quickly tested.

## ACKNOWLEDGEMENTS

We thank E. Barr, J-P. Macquart and an anonymous referee for extensive helpful comments which have hugely improved the quality of this manuscript. EFK and EP acknowledge the support of the Australian Research Council Centre of Excellence for All-sky Astrophysics (CAASTRO), through project number CE110 001 020.

## REFERENCES

- Bannister K. W., Madsen G. J., 2014, *MNRAS*, 440, 353  
 Burke-Spolaor S., Bannister K. W., 2014, *ApJ*, 792, 19  
 Cordes J. M., Lazio T. J. W., 2002, preprint ([astro-ph/0207156](https://arxiv.org/abs/astro-ph/0207156))  
 Cordes J. M., McLaughlin M. A., 2003, *ApJ*, 596, 1142  
 Dennison B., 2014, *MNRAS*, 443, L11  
 Fender R. P., 2015, *Proc. Sci., Advancing Astrophysics with the Square Kilometre Array*, in press  
 Gao H., Li Z., Zhang B., 2014, *ApJ*, 788, 189  
 Inoue S., 2004, *MNRAS*, 348, 999  
 Ioka K., 2003, *ApJ*, 598, L79  
 Keane E. F., McLaughlin M. A., 2011, *Bull. Astron. Soc. India*, 39, 333  
 Keane E. F., Ludovici D. A., Eatough R. P., Kramer M., Lyne A. G., McLaughlin M. A., Stappers B. W., 2010, *MNRAS*, 401, 1057  
 Keane E. F., Kramer M., Lyne A. G., Stappers B. W., McLaughlin M. A., 2011, *MNRAS*, 415, 3065  
 Keane E. F., Stappers B. W., Kramer M., Lyne A. G., 2012, *MNRAS*, 425, L71  
 Lorimer D. R., Bailes M., McLaughlin M. A., Narkevic D. J., Crawford F., 2007, *Science*, 318, 777  
 McQuinn M., 2014, *ApJ*, 780, L33  
 Manchester R. N. et al., 2001, *MNRAS*, 328, 17  
 Petroff E. et al., 2014a, *ApJ*, 789, L26  
 Petroff E. et al., 2014b, *MNRAS*, preprint ([arXiv:1412.0342](https://arxiv.org/abs/1412.0342))  
 Spitler L. G. et al., 2014, *ApJ*, 790, 101  
 Staveley-Smith L. et al., 1996, *PASA*, 13, 243  
 Thornton D. et al., 2013, *Science*, 341, 53  
 Wright E. L., 2006, *PASP*, 118, 1711  
 Zhou B., Li X., Wang T., Fan Y.-Z., Wei D.-M., 2014, *Phys. Rev. D*, 89, 107303

This paper has been typeset from a  $\text{\TeX}/\text{\LaTeX}$  file prepared by the author.